Keratinocyte-specific stat3 heterozygosity impairs development of skin tumors in human papillomavirus 8 transgenic mice

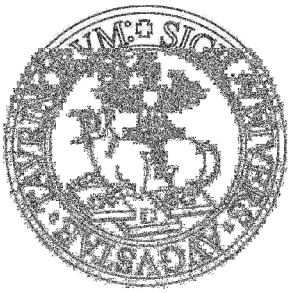

Keratinocyte-specific STAT3 heterozygosity impairs development of skin tumors in HPV8 transgenic mice

Marco De Andrea,[1,2] Massimo Rittà,[1,2] Manuela M. Landini,[2] Cinzia Borgogna,[2] Michele Mondini,[2] Florian Kern,[3] Karin Ehrenreiter,[3] Manuela Baccarini,[3] Gian Paolo Marcuzzi,[4] Sigrun Smola,[4,5] Herbert Pfister,[4] Santo Landolfo,[1] and Marisa Gariglio[2]

[1]Department of Public Health and Microbiology, Medical School of Turin, Turin, Italy;
[2]Department of Clinical and Experimental Medicine, Medical School of Novara, Novara, Italy;
[3]Max F. Perutz Laboratories, University of Vienna, Vienna, Austria;
[4]Institute of Virology, Center of Molecular Medicine, University of Cologne, Cologne, Germany
[5]Institute of Virology, Saarland University, Homburg/Saar, Germany

Running Title: Stat3 function in HPV8-induced skin carcinogenesis

Key Words: Stat3, Human Papillomavirus, Non-Melanoma Skin Cancer, Conditional Knockout

Grant support: Regione Piemonte ('Ricerca Sanitaria Finalizzata' 2008, 2008bis and 2009 to MDeA, MM, SL and MG), Italian Ministry for University and Research MIUR (PRIN 2008 to SL and MG, and FIRB - Futuro in Ricerca 2008 to MDeA), and Fondazione Banca Popolare di Novara BPN (to MG).

Corresponding author: Marisa Gariglio, Department of Clinical and Experimental Medicine, Medical School of Novara, via Solaroli 17, 28100 Novara, Italy. Phone: +39-0321-660649; Fax: +39-0321-620421. E-mail: gariglio@med.unipmn.it.

Footnotes

M. De Andrea and M. Rittà contributed equally to this study

Abstract

Human Papillomaviruses (HPVs) of the genus beta are thought to play a role in human skin cancers, but this has been difficult to establish using epidemiological approaches. To gain insight into the transforming activities of β-HPV, transgenic mouse models have been generated that develop skin tumors. Recent evidence suggests a central role of signal transducer and activator of transcription 3 (Stat3) as a transcriptional node for cancer cell-autonomous initiation of a tumor-promoting gene signature associated with cell proliferation, cell survival, and angiogenesis. Moreover, high levels of phospho-Stat3 (pStat3) have been detected in tumors arising in HPV8-CER transgenic mice. In this study, we investigate the in vivo role of Stat3 in HPV8-induced skin carcinogenesis by combining our established experimental model of HPV8-induced skin cancer with epidermis-restricted Stat3 ablation. Stat3 heterozygous epidermis was less prone to tumorigenesis than wild-type epidermis. Three of the 23 $Stat3^{+/-}$:HPV8 animals (13%) developed tumors within 12 weeks of life, while 54.3% of $Stat3^{+/+}$:HPV8 mice already exhibited tumors in the same observation period (median age for tumor appearance: 10 weeks). The few tumors that arose in the $Stat3^{+/-}$:HPV8 mice were benign and never progressed to a more malignant phenotype. Collectively, these results offer direct evidence of a critical role for Stat3 in HPV8-driven epithelial carcinogenesis. Our findings imply that targeting Stat3 activity in keratinocytes may be a viable strategy to prevent and treat HPV-induced skin cancer.

Introduction

Human Papillomaviruses (HPVs) are small DNA tumor viruses that are strictly epitheliotropic and infect keratinocytes at a wide range of body sites. Over 120 different types of HPV have been identified to date, classified into several phylogenetic groups (1). Of these, the α-genus HPVs, associated with infections of mucosal epithelia, are the best characterized and can be grouped into 'low-risk' and 'high-risk' types depending on the relative tendency of the virus-induced neoplasm to undergo malignant progression (2, 3).

Beta-HPVs are associated with infections of the skin and comprise a similarly large group of HPVs (4, 5). They cause widespread inapparent or asymptomatic infections in the general population, and children become infected at an early age. In immunosuppressed patients and individuals suffering from Epidermodysplasia Verruciformis (EV) (6, 7), a rare inherited skin disease, these viruses can spread unchecked and have been implicated in the development of non-melanoma skin cancer (NMSC), particularly in sun-exposed areas (8).

The causal relationship between HPV infection and Squamous Cell Carcinoma (SCC) of the genital tract is well established. HPV β-genotypes are suspected of playing a role in skin cancers, but this has been difficult to establish using epidemiological approaches due to the ubiquitous prevalence of these viruses in the general population and their absence in some cancers (4, 9).

Transgenic mouse models have been used to gain insight into the transforming activities of β-HPV. Expression of the complete early genome region (CER) of HPV8 in transgenic mice was found to be sufficient for the spontaneous development of NMSC (10). In addition, our group has demonstrated the intrinsic oncogenic potential of HPV8 E2 (11) and HPV8 E6 (12) using transgenic animals. Once more using transgenic technology, several mouse lines have been developed that express E6/E7 from other β-genotypes, such as HPV38 (13) and HPV20 (14), but HPV8 has so far been the only cutaneous HPV type found to induce skin cancer completely on its own in the absence of any additional co-carcinogenic treatment.

Signal transducer and activator of transcription 3 (Stat3) is a transcription factor that belongs to a family of cytoplasmic proteins that participate in normal cellular responses to cytokines and growth factors (15). Activation of a wide variety of cell surface receptors leads to the tyrosine phosphorylation of Stat3 (pStat3) which then dimerizes and translocates to the nucleus, where it modulates the expression of target genes that are involved in various physiological functions, including cell cycle regulation, apoptosis and cell differentiation (16, 17). Knocking Stat3 out of the germline results in embryonic lethality (18), implying that Stat3 has global and critical effects upon development. Keratinocyte-specific Stat3-null mice demonstrate that Stat3 plays a pivotal role in skin remodeling since the hair cycle and wound healing processes are found to be severely

compromised in these mice (19). Chan and colleagues (20) went on to demonstrate that these knockouts are completely resistant to the two-stage carcinogenesis regimen using 7,12-dimethylbenz(a)anthracene (DMBA) as the initiator and TPA as the promoter, thus indicating that Stat3 is essential for the development of chemically induced skin tumors in mice. In addition, they found that Stat3-deficient keratinocytes were highly sensitive to UVB-induced apoptosis, whereas overexpression of Stat3 or expression of a Stat3C transgene protected keratinocytes from UVB-induced apoptosis (21-24). All in all, these findings clearly demonstrate that Stat3 plays a critical role in both two-stage chemical-induced and physical UVB-mediated skin carcinogenesis.

In this study, we address the *in vivo* role of Stat3 in HPV8-induced skin carcinogenesis using HPV8-CER transgenic mice crossed with keratinocyte-specific Stat3-disrupted mice, and report the remarkable observation that heterozygous mice, carrying only one Stat3 functional allele, respond poorly to proliferation induced by viral oncogenic proteins. The present study shows, for the first time, that the reduced expression of the Stat3 gene has a significant impact upon skin tumor development in this mouse model of viral carcinogenesis and provides a rationale for evaluating the potential use of Stat3 inhibitors in the prevention and treatment of tumors associated with β-HPV infection.

Materials and Methods

Generation of transgenic mice. K14-HPV8/FVB transgenic mice have been previously described (10). K5Cre-Stat3$^{wt/LoxP}$ mice were obtained by crossing K5Cre transgenic mice expressing Cre recombinase under the control of the keratinocyte specific Keratin 5 promoter (25, 26) with Stat3$^{LoxP/LoxP}$ animals previously described (27; kindly provided by Dr Levy, New York University). Mice were housed in accordance with The Guide for the Care and Use of Laboratory Animals.

Genotyping of progeny. Genomic DNA was isolated from tail biopsies of 7-day-old mice using the QIAmp Tissue kit (Qiagen) or from 0.5% dispase II (Roche) and trypsin (Sigma) treated full-thickness skin. PCR analysis to detect Stat3 wild-type, floxed or null alleles was performed using primers designed to amplify the DNA sequence between exons 15-22 (Fig. 1A). Briefly, DNA (~0.3μg) was incubated with two forward primers: "A" (5'-CAGAACCAGGCGGCTCGTGTGCG-3'; specific for intron 21) and "C" (5'-GAAGGCAGGTCTCTCTGGTGCTTC-3'; specific for intron 15) and one reverse primer "B" (5'GCTGCCAACAGCCACTGCCCCAG-3'; specific for intron 21) ([Final] = 0.25μM) in a final volume of 25 μl using REDTaq ReadyMix PCR Reaction Mix (Sigma). PCR reactions were performed on a MJ PTC-200 thermal cycler (Bio-Rad) using the following protocol: 94°C for 2 min; 35 cycles of: 94°C for 45 sec, 58°C for 40 sec and 72°C for 1 min, and a final extension period at 72°C for 7 min. PCR products were separated by 2% agarose-TAE gel electrophoresis and ethidium bromide staining was used to detect the separated bands. Stat3 band sizes were expected to be: ~140bp for the wild-type allele; ~240bp for the floxed allele; and ~400bp for the null allele. The PCR protocols used for the Cre and HPV8 transgenes was previously described (10, 25).

Preparation of epidermal cell lysates and Western Blot analysis. Mice were sacrificed by cervical dislocation. The dorsal skin of the mice was shaved and depilated; the skin was then excised and the epidermis peeled away from the dermis following overnight treatment with 0.5% dispase II (Roche) and then homogenized in lysis buffer containing 100 mM Tris-HCl (pH 6.8), 1.25% β-mercaptoethanol, 4% sodium dodecyl sulfate (SDS), 1% Bromophenol blue, 10% Glycerol, 25 μL/mL Protease Inhibitor Cocktail (Sigma) and 1μL/100μL Phosphatase Inhibitor Cocktail 2 (Sigma). Supernatants were analyzed for protein concentration using the QuantiPro BCA Assay Kit (Sigma). Three whole-cell lysates were pooled, fractionated on 8-12% SDS-PAGE and transferred to PVDF membranes (Millipore). The following primary antibodies were used: Stat3 and pStat3 (Cell Signaling Technology, clones 124H6 and D3A7; 1:1000 and 1:2000); Vimentin (Sigma; clone V9; 1:3000); PanEpithelial Keratin (Progen Biotechnik, clone Ks 5+8.22/C 22; 1:300); Actin (Chemicon, clone C4; 1:3000).

Histological and immunohistochemical analysis of the skin. Sections (4μm thick) were cut from formalin-fixed and paraffin embedded skin, deparaffinized, and rehydrated using standard procedures. Serial sections were either stained with hematoxylin/eosin (H&E) or used for immunostaining using primary antibodies raised against the following proteins: keratin 5 (K5) (Covance, clone AF138; 1:500); keratin 10 (K10) (Covance; 1:1000); Proliferating Cell Nuclear Antigen (PCNA) (Santa Cruz Biotechnology; 1:4000); Stat3 (Cell Signaling Technology; 1:100); pStat3 (Cell Signaling Technology; clone D3A7; 1:50). Endogenous peroxidase activity was blocked by treatment with 3% hydrogen peroxide in 1X PBS for 10 minutes. Antigen unmasking was performed by microwaving the sections for 10 minutes in 10 mM citrate buffer (pH 6.0) for K5, K10, Stat3, and PCNA antibodies, and for pStat3 in 1 mM EDTA (pH 8.0) for 12 minutes. For K5, K10, Stat3, and PCNA antibodies, we used the biotinylated universal anti-rabbit/mouse secondary antibody followed by incubation with the streptavidin-horseradish peroxidase complex (Vector Laboratories). For revelation of pStat3 we used the DAKO EnVision Plus Detection System (Dako). Bound antibodies were visualized by 3,3'diaminobenzidine, counterstained with Mayer's Haematoxylin, and mounted with VectaMount permanent mounting medium (Vector Laboratories).

Evaluation of epidermal thickness, PCNA and pStat3 staining. Paraffin sections were stained with H&E and the epidermal thickness was measured by using Image-Pro Plus 6.0 software technology. For the quantification of PCNA- and pStat3-positive staining cells, ten random areas were selected for each mouse. The number of cells demonstrating positive labelling and the total number of cells counted (1000) were recorded by using Image-Pro Plus 6.0 software technology. An average percentage was then calculated based on the total number of cells and the number of positive staining cells from each set of 10 fields counted.

Quantitative real-time RT-PCR (qRT-PCR). For the determination of E6 and E7 gene expression levels, RNA was extracted from 0.5% dispase II and trypsin treated full-thickness skin using the NucleoSpin RNA extraction Kit (Macherey-Nagel) and treated with DNase-I (Sigma). Total RNA (1μg) was retro-transcribed using the ImProm-II Reverse Transcription System (Promega). SYBR-green I qRT-PCR was performed and the housekeeping gene *β-actin* was used to normalize the variation in cDNA levels. Each standard curve was constructed using values from serially diluted HPV8-negative mouse cDNA mixed with plasmid encoding E6/E7 of HPV8. Wild-type mouse cDNA was amplified to verify the absence of genomic contaminations. SYBR-green I amplifications were performed as previously described (10) using the GeneAmp 7000 Sequence Detection System (Applied Biosystems).

Statistical analysis. All statistical tests were performed using GraphPad Prism version 5.00 for Windows. Two-way ANOVA followed by Bonferroni post-tests were used to analyze whether the differences in mean epidermal thickness and PCNA proliferating indices were affected by the Stat3 genotype. One-way ANOVA followed by the Bonferroni post-test was used to analyze the differences in the p-Stat3 immunohistochemical score between genotypes. Finally, the Fischer's exact test was used to compare tumor incidences between mouse genotypes.

Results and Discussion

Phenotypes of skin-specific Stat3 knockout mice expressing HPV8 early genes. Mice with epidermis-restricted Stat3 deletion (K5Cre-Stat3$^{wt/loxP}$ mice) were mated with animals in which HPV8 early genes expression was driven by the K14 promoter (K14-HPV8 mice). The resulting K5Cre-Stat3$^{wt/LoxP}$/K14-HPV8 mice were then backcrossed with parental K14-HPV8 mice for 6 generations to yield a pure FVB/N background, and finally interbred to generate all the possible genotypes detailed in Table 1.

Since K5 and K14 proteins are expressed in the same cell lineages (28), including the basal keratinocytes of the interfollicular epidermis and the outer root sheath (namely, the follicular keratinocytes), the Stat3$^{-/-}$:HPV8 mice have a constitutive overexpression of the HPV8 early genes in the same cells as those carrying the Cre-mediated Stat3 ablation. Genotyping of the Stat3 gene for both alleles was carried out by genomic PCR (Fig. 1A and 1B) and the efficiency and specificity of the Cre-mediated Stat3 disruption was determined by Western blot analysis (Fig. 1C). Stat3 protein levels were dramatically reduced in homozygous mice as a consequence of the Cre-mediated Stat3 gene disruption, while levels were reduced by approximately 50% in heterozygous mice compared to the parental mice. As expected, the epidermal lysates contained the epithelial specific marker pan-keratin, but not the fibroblast specific marker vimentin confirming their purity.

Soon after birth, both Stat3$^{-/-}$ and Stat3$^{-/-}$:HPV8 mice started to fail (Fig. 2A). Within postnatal day 10 (PD10), they exhibited lethargy, retarded development, spontaneous wounds, and sparse hair development. By PD12-15, they developed patches of rough skin with scales and crusts and invariably died prematurely. Most homozygous mice died between 20 and 30 days after birth irrespective of whether they possessed the HPV8 transgenes or not; a few survived longer, but for no more than 40 days. Previous reports have shown that the K5 gene is expressed not only in the epidermis, but also in the esophagus and stomach (25, 29, 30); Stat3 disruption would therefore also occur in these tissues as a consequence of K5-driven Cre expression. Indeed, no food was found in the stomach of the dead mice and the esophagus was smaller in mutant mice than in wild-type (WT) mice (data not shown), suggesting that death was primarily caused by a defect in food intake as a result of esophagus dysfunction. The fact that the Stat3$^{-/-}$ mice have a high morbidity rate and short life span meant that it was not possible to investigate the tumorigenic effects of HPV8 early genes in these mice. In contrast, mice carrying a single functional Stat3 allele did not show any overt phenotype or gross modifications of the skin, and lived a normal average life span. These phenotype results are similar to those reported by Sano *et al.* (19), but in our mouse model they appear earlier and with stronger severity. The Cre-LoxP system used by Sano and colleagues specifically removed the tyrosine residue essential for phosphorylation (Tyr705) and the MAP-kinase recognition site

spanning exons 21-22 within the Stat3 gene, deleting full-length Stat3 but allowing the expression of truncated form with possible residual activity. In contrast, the gene disruption strategy used in our study, resulting in the total deletion of exons 16 to 21, completely abolished Stat3 expression, thus justifying the stronger phenotype observed in our mouse model.

Histological analysis and measurement of the epidermal thickness of the skin obtained from healthy areas of the different genotypes (4 mice for each genotype) at about one month of age revealed marked differences between WT and Stat3 null mice. The epidermis in the null mice was so thin that it was not possible to measure it (Fig. 2B and 2E), and there was no increase in epidermal layer thickness as a consequence of viral oncoproteins expression. Severely distorted hair follicles could be observed that formed cysts filled with lamellar and eosinophilic material in the upper dermis, particularly in the $Stat3^{-/-}$:HPV8 mice. This alteration of hair architecture has been previously reported and is related to the lack of Stat3 in the outer root sheath cells (19). In contrast, both stratification of the squamous epithelia of the skin and hair follicle development were normal in heterozygous mice. The epidermis of nontransgenic $Stat3^{+/-}$ mice was slightly thinner than that of $Stat3^{+/+}$ and was not significantly thicker in the $Stat3^{+/-}$:HPV8. In contrast, the total thickness of the epidermis of $Stat3^{+/+}$:HPV8 mice was approximately doubled compared to their nontransgenic wild-type counterparts and significantly thicker than that of $Stat3^{+/-}$:HPV8 mice. Proliferation was also evaluated by PCNA immunostaining. Consistent with the results observed by measuring epidermal thickness, PCNA staining was not detectable in the epidermis of Stat3 null mice, nor was it present in the $Stat3^{-/-}$:HPV8 transgenic mice (Fig. 2C). The number of PCNA-positive cells was significantly greater in the epidermis of $Stat3^{+/+}$:HPV8 compared with their nontransgenic counterparts, and no significant difference was found between $Stat3^{+/-}$:HPV8 mice and the nontransgenic $Stat3^{+/-}$ mice (Fig. 2F). Here again the number of PCNA-positive cells was significantly greater in $Stat3^{+/+}$:HPV8 mice compared to $Stat3^{+/-}$:HPV8 mice.

Keratinocyte-specific ablation of Stat3 expression was confirmed by immunohistochemistry. As shown in Fig. 2D, strong positive immunostaining was observed in all layers of the epithelium in both $Stat3^{+/+}$ and $Stat3^{+/+}$:HPV8 skin sections. According to the protein levels detected by Western blotting (Fig. 1C), Stat3 expression was significantly reduced in heterozygous mice in comparison with WTs, yet remained present in all layers of the epithelium. As expected, Stat3 staining was absent in the skin of $Stat3^{-/-}$ mice in both interfollicular epidermis and follicular keratinocytes. Collectively, these findings indicate that, even in nonlesional skin of heterozygous mice, the reduction of Stat3 protein levels significantly affects the degree of hyperplasia induced by HPV8 oncoproteins.

Stat3 heterozygosity significantly decreases HPV8-induced tumor formation. From our initial characterization of the different mouse genotypes, to our surprise we noted that spontaneous skin lesions in a sample of $Stat3^{+/-}$:HPV8 mice did not occur during an observation period that spanned the first 3 months of life. On account of this finding, we monitored spontaneous tumor formation over a 52-week period in a larger cohort of $Stat3^{+/-}$:HPV8 mice (n=23) and $Stat3^{+/+}$:HPV8 mice (n=81). All animals were followed for a minimum of 12 weeks. The Kaplan-Meier plot of the tumor-free state as a function of time showed statistically significant differences between the two groups (Fig. 3), with a disease-free survival greatly enhanced in the Stat3 heterozygous mice. The median age for tumor appearance was 10 weeks in $Stat3^{+/+}$:HPV8 mice (Log-rank test; $p<0.0001$). Indeed, only 3 of the 23 $Stat3^{+/-}$:HPV8 mice (13%) displayed tumor formation within 12 weeks of life, while in the same period 44 of the 81 $Stat3^{+/+}$:HPV8 had already developed one or more tumors (54.3%) (Table 2). No influence of gender upon tumor development was detected. The macroscopic appearance and the localization of the skin lesions in $Stat3^{+/+}$:HPV8 were identical to the skin tumors previously described in HPV8-CER mice (10). These lesions progressed continuously (15.8% of tumors progressed to malignancy) and never regressed. Interestingly, in Stat3 heterozygous mice all the tumors were benign as they did not exhibit any signs of ulceration, although they developed in the same location and with the same initial morphology as those in $Stat3^{+/+}$:HPV8 mice. Indeed, they remained circumscribed and reduced in size for the entire observation period, whereas lesions in the $Stat3^{+/+}$:HPV8 mice became more hyperkeratotic and spread diffusely. Overall, skin lesions in $Stat3^{+/-}$:HPV8 mice did not progress neither did they show any signs of regression. Since 3 of the 5 $Stat3^{+/-}$:HPV8 mice that developed skin lesions were sacrificed for immunohistochemical analysis, sample numbers were too small to conclude with statistics that they would not have progressed to malignancy as occurred in the WT counterparts. It is worth noting however that the two $Stat3^{+/-}$:HPV8 mice that lived longer than the observation period (12 months) never developed any signs of malignant progression. Collectively, these observations show that the susceptibility to HPV8-induced skin tumor development is significantly reduced under conditions of Stat3 heterozygosity.

To verify that the results obtained were not related to different transgene expression levels between the WT and heterozygous mice, the levels of HPV8-E6 and HPV8-E7 mRNA in total RNA isolated from epidermal lysates of non-lesional skin in $Stat3^{+/+}$:HPV8 and $Stat3^{+/-}$:HPV8 animals (three of each genotype) were measured in duplicate by qRT-PCR. Epidermal expression levels of the HPV8-E6 and HPV8-E7 mRNAs did not differ between mice of the same genotype or between mice of different genotype and were highest for E7 as previously reported. The mean range values ($\pm$ SEM) were 0.22 ± 0.01 *vs.* 0.16 ± 0.06 for E6 transcripts in $Stat3^{+/+}$:HPV8 *vs.* $Stat3^{+/-}$:HPV8

mice, and 0.43 ± 0.12 *vs*. 0.47 ± 0.24 for E7 transcripts in Stat3$^{+/+}$:HPV8 *vs*. Stat3$^{+/-}$:HPV8 respectively. As a further control, the HPV8 transgene copy number was determined by quantitative real-time PCR in tumor-bearing mice from either Stat3$^{+/+}$:HPV8 or Stat3$^{+/-}$:HPV8 and compared with tumor-free mice from both groups and Stat3$^{+/+}$:HPV8 mice showing SCC progression. The proportion of hemi (30%) or homozygous (70%) animals for the HPV8 transgene was equally distributed, excluding the possibility that the results obtained were due to accumulation of HPV8 homozygous mice in a specific group during interbreeding (data not shown).

*Assessment of Stat3 status, tumor growth, and proliferation***.** As stated above and shown in the representative example reported in Fig. 4A, lesions in 15.8% of Stat3$^{+/+}$:HPV8 mice spontaneously progressed from papilloma to carcinoma over a time period of 8 to 24 weeks from their onset, at an average age of 17.3 weeks. Tumors arising in Stat3$^{+/+}$:HPV8 mice were mostly ulcerated and invasive, features of malignancy. This progression was never observed in Stat3$^{+/-}$:HPV8 mice where lesions were limited in size and self-contained, thus indicative of benign papillomas, even at older ages (e.g. 20 weeks), as reported in the example of Fig. 4 right column. The histopathological analysis confirmed they were all benign papillomas containing an endophytic component that grew towards the dermis (Fig. 4A central right). They possessed concentrically keratinized structures, a common feature of β-HPV-induced hyperplasia. Even in older Stat3$^{+/-}$:HPV8 mice, these lesions never showed signs of early malignant transformation, such as hyperchromatic nuclei, loss of stratification, and mitotic figures in the upper cell layers; such features were commonly detected in the lesions obtained from the Stat3$^{+/+}$:HPV8 mice of the same age (data not shown). Papillomas arising in Stat3$^{+/+}$:HPV8 mice displayed the same histological features described for Stat3$^{+/-}$:HPV8. In contrast, carcinomas arising in Stat3$^{+/+}$:HPV8 mice showed loss of epithelium stratification, with markedly atypical cells, and infiltrative growth of tumor cells into the underlying connective tissue (Fig. 4A, central column). Collectively, these results demonstrate that a reduction in Stat3 protein levels strongly affects the progression of skin carcinogenesis.

Having established that Stat3 plays a crucial role in keratinocyte transformation induced by HPV8 early genes in vivo, we determined whether there had been any impact on the status of Stat3 phosphorylation. Following phosphorylation, Stat3 translocates to the nucleus, becomes transcriptionally active, and promotes the development of epidermal hyperplasia and/or malignant tumors in mice (22). Immunohistochemical analysis revealed keratinocyte-specific nuclear localization of the tyrosine-phosphorylated (activated) form of Stat3 (pStat3) in all the lesions analyzed from both Stat3$^{+/+}$:HPV8 and Stat3$^{+/-}$:HPV8 mice (Fig. 4A lower row) in the basal and suprabasal layers. In non-lesional skin of both genotypes, pStat3 nuclear localization was restricted to just a few cells in the basal proliferating layer of the epidermis (data not shown). The number of

pStat3-positive cells was significantly higher in the papillomas arising in both the $Stat3^{+/+}$:HPV8 and $Stat3^{+/-}$:HPV8 mice compared with non-lesional epidermis from both genotypes, and moreover, the scores were similar in the papillomas (Fig. 4B). In $Stat3^{+/+}$:HPV8 mice, scores for pStat3 nuclear staining were higher for carcinomas than for papillomas. Upregulation of the Stat3 protein as well as its activation in the tumors that arose in both WT and heterozygous mice was also confirmed by immunoblotting (Fig. 4C). Thus, these results clearly indicate that Stat3 activation is associated with HPV8-induced hyperproliferation and suggest that a requisite level of activated Stat3 must accumulate for a neoplasia to develop.

In addition, in order to analyze the proliferative status of the skin cells, nuclei were stained for the presence of PCNA (Fig. 5, upper row). Expression of the viral oncoproteins increased the number of PCNA-positive cells in the suprabasal layers of papillomas from both $Stat3^{+/+}$:HPV8 and $Stat3^{+/-}$:HPV8 mice, although in heterozygous mice the staining was more disorganized with a higher number of positive cells in the inner suprabasal layers. As expected, PCNA expression in carcinomas from $Stat3^{+/+}$:HPV8 mice extended all the way through the dysplastic epidermis.

To assess whether the differences in HPV8-induced tumor progression in $Stat3^{+/+}$ vs $Stat3^{+/-}$ were associated with the degree of tumor cell differentiation, we evaluated the expression of a marker of suprabasal differentiated keratinocytes (K10) and of undifferentiated basal (K5) compartments of the epidermis. In control epidermis, K10 is expressed by postmitotic keratinocytes in the suprabasal layers during normal differentiation (data not shown). As shown in Figure 5 central row, the hyperplasia of suprabasal keratinocytes induced by HPV8 oncoproteins in papillomas and carcinomas from $Stat3^{+/+}$:HPV8 mice was paralleled by a strong reduction of K10 expression in the inner suprabasal layers; expression was shifted outwards, sporadically observed in the flattened cells positioned just beneath the malformed corny layer. A similar pattern was observed in the papillomas from heterozygous mice, although clusters of K10-positive cells were still present in the more differentiated areas of the concentrically keratinized structures. The increased proliferation and hyperplasia of suprabasal keratinocytes induced by viral oncoproteins expression was accompanied by the accumulation of less differentiated suprabasal cells. This was indicated by the persistent expression of the basal marker K5 in the suprabasal layers and its retention throughout the hyperplastic epidermis (Fig. 5, lower row). It is also worth mentioning that K5-positive invading keratinocytes were present in the dermal compartment of $Stat3^{+/+}$:HPV8 papillomas, confirming that these lesions are malignant, but never in $Stat3^{+/-}$:HPV8 papillomas.

The physiological importance of Stat3 in the maintenance of skin integrity as well as the pathogenesis of skin diseases has been described in many experimental settings, including *in vitro* cell culture systems (19, 21, 31) and skin specific Stat3-deficient mice obtained by conditional gene

targeting (19). In the current study, by using a different Cre-LoxP strategy to that used by Sano *et al.* (19), we have confirmed the fundamental role of Stat3 in the maintenance of hair growth and epidermal homeostasis. Indeed, histology of the skin from $Stat3^{-/-}$ mice revealed severe epidermal loss and alteration of hair architecture.

In order to comprehend further the biological functions of Stat3, we addressed the question of whether more subtle changes in Stat3 expression could also influence tumor development in our experimental setting. $Stat3^{+/-}$ mice appeared identical to their $Stat3^{+/+}$ littermates: they had no apparent abnormalities and lived a normal average life span. However, comparing tumor yields in $Stat3^{+/+}$:HPV8 versus $Stat3^{+/-}$:HPV8 mice revealed surprisingly highly significant effects of Stat3 heterozygosity upon skin tumor susceptibility triggered by HPV8 early genes. Despite the rather modest effect upon Stat3 expression, the effect upon tumor development was considerable: significantly fewer tumors were produced in $Stat3^{+/-}$:HPV8 mice compared to $Stat3^{+/+}$:HPV8 mice, a finding that provides genetic proof of the notion that even a relatively modest reduction in Stat3 expression can indeed affect tumor development in a rather profound manner. Moreover, all the tumors in the Stat3 heterozygous mice showed signs of being benign and never progressed to a more malignant phenotype. The rate and extent of keratinocyte proliferation, the delay in keratinocyte differentiation, and the level of pStat3-positively stained nuclei were similar between papillomas arising in $Stat3^{+/+}$:HPV8 and $Stat3^{+/-}$:HPV8 mice. These findings indicate that a certain amount of activated Stat3 is necessary to achieve uncontrolled proliferation and therefore only cells that display the appropriate levels of Stat3 will be capable of proliferating in response to the viral oncoproteins. Our findings support the emerging concept that differences in tissue expression levels of proteins involved in cell cycle control, resulting from either overexpression or reductions, can affect tumor susceptibility (32). Furthermore, a surprising number of complicated clinical manifestations associated with genetic syndromes are known to be due to mutations in genes encoding transcription factors (33). The mechanism through which transcription factor defects cause disease is often heterozygosity, indicating that half-normal levels of many transcription factors are simply not enough to provide normal function (34).

A causal link between Stat3 ablation and reduction in tumor yield was also demonstrated by Bollrath and colleagues (35) in their $Stat3^{\Delta IEC}$ mice where Stat3 was selectively knocked-out in all the epithelial cell lineages of the intestine. The $Stat3^{\Delta IEC}$ mice were generated by a Cre-LoxP strategy expressing Cre recombinase under the control of the intestine-specific villin gene promoter. Exposure of these $Stat3^{\Delta IEC}$ mice to the colitis-associated cancer (CAC) challenge revealed they were almost completely protected from the development of tubular adenomas induced by the colonotropic mutagen azoxymethane (AOM). Consistent with our findings, the few polypoid

lesions protruding into the lumen that developed in a small proportion of $Stat3^{\Delta IEC}$ mice were markedly reduced in size.

Collectively, these studies provide for the first time evidence of a critical role of Stat3 in the experimental mouse model of HPV8-induced epithelial carcinogenesis and suggest that targeting Stat3 in keratinocytes may be a viable strategy for the prevention and treatment of HPV-induced skin cancer.

Acknowledgments

We would like to thank Dr. David Levy from New York University for kindly providing the $Stat3^{LoxP/LoxP}$ mice, Dr. Roberto Chiarle from the University of Turin for his helpful discussions. CB is on leave of permit at the NIMR in London on a fellowship from FEMS.

References

1. de Villiers EM, Fauquet C, Broker TR, Bernard HU, zur Hausen H. Classification of papillomaviruses. Virology 2004;324:17-27

2. Snijders PJ, Steenbergen RD, Heideman DA, Meijer CJ. HPV-mediated cervical carcinogenesis: concepts and clinical implications. J Pathol 2006;208:152-64

3. zur Hausen H. Papillomaviruses in the causation of human cancers - a brief historical account. Virology 2009;384:260-5

4. Akgul B, Cooke JC, Storey A. HPV-associated skin disease. J Pathol 2006;208:165-75

5. Nindl I, Gottschling M, Stockfleth E. Human papillomaviruses and non-melanoma skin cancer: basic virology and clinical manifestations. Dis Markers 2007;23:247-59

6. Zavattaro E, Azzimonti B, Mondini M, et al. Identification of defective Fas function and variation of the perforin gene in an epidermodysplasia verruciformis patient lacking EVER1 and EVER2 mutations. J Invest Dermatol 2008;128:732-5

7. Dell'oste V, Azzimonti B, De Andrea M, et al. High beta-HPV DNA Loads and Strong Seroreactivity Are Present in Epidermodysplasia Verruciformis. J Invest Dermatol 2009; 129:1026-34

8. Bouwes Bavinck JN, Plasmeijer EI, Feltkamp MC. Beta-papillomavirus infection and skin cancer. J Invest Dermatol 2008;128:1355-8

9. Pfister, H. Chapter 8: Human papillomavirus and skin cancer. J Natl Cancer Inst Monogr*:* 52-56, 2003

10. Schaper ID, Marcuzzi GP, Weissenborn SJ, et al. Development of skin tumors in mice transgenic for early genes of human papillomavirus type 8. Cancer Res 2005;65:1394-400

11. Pfefferle R, Marcuzzi GP, Akgul B, et al. The human papillomavirus type 8 E2 protein induces skin tumors in transgenic mice. J Invest Dermatol 2008;128:2310-5

12. Marcuzzi GP, Hufbauer M, Kasper HU, Weissenborn SJ, Smola S, Pfister H. Spontaneous tumour development in human papillomavirus type 8 E6 transgenic mice and rapid induction by UV-light exposure and wounding. J Gen Virol 2009;90:2855-64

13. Dong W, Kloz U, Accardi R, et al. Skin hyperproliferation and susceptibility to chemical carcinogenesis in transgenic mice expressing E6 and E7 of human papillomavirus type 38. J Virol 2005;79:14899-908

14. Michel A, Kopp-Schneider A, Zentgraf H, Gruber AD, de Villiers EM. E6/E7 expression of human papillomavirus type 20 (HPV-20) and HPV-27 influences proliferation and differentiation of the skin in UV-irradiated SKH-hr1 transgenic mice. J Virol 2006;80:11153-64

15. Zhong Z, Wen Z, Darnell JE Jr. Stat3: a STAT family member activated by tyrosine phosphorylation in response to epidermal growth factor and interleukin-6. Science. 1994 Apr 1;264(5155):95-8

16. Levy DE, Darnell JE, Jr. Stats: transcriptional control and biological impact. Nat Rev Mol Cell Biol 2002;3:651-62

17. Aggarwal BB, Kunnumakkara AB, Harikumar KB, et al. Signal transducer and activator of transcription-3, inflammation, and cancer: how intimate is the relationship? Ann N Y Acad Sci 2009;1171:59-76

18. Takeda K, Noguchi K, Shi W, et al. Targeted disruption of the mouse Stat3 gene leads to early embryonic lethality. Proc Natl Acad Sci U S A 1997;94:3801-4

19. Sano S, Itami S, Takeda K, et al. Keratinocyte-specific ablation of Stat3 exhibits impaired skin remodeling, but does not affect skin morphogenesis. Embo J 1999;18:4657-68

20. Chan KS, Sano S, Kiguchi K, et al. Disruption of Stat3 reveals a critical role in both the initiation and the promotion stages of epithelial carcinogenesis. J Clin Invest 2004;114:720-8

21. Sano S, Chan KS, Kira M, et al. Signal transducer and activator of transcription 3 is a key regulator of keratinocyte survival and proliferation following UV irradiation. Cancer Res 2005;65:5720-9

22. Chan KS, Sano S, Kataoka K, et al. Forced expression of a constitutively active form of Stat3 in mouse epidermis enhances malignant progression of skin tumors induced by two-stage carcinogenesis. Oncogene 2008;27:1087-94

23. Kataoka K, Kim DJ, Carbajal S, Clifford JL, DiGiovanni J. Stage-specific disruption of Stat3 demonstrates a direct requirement during both the initiation and promotion stages of mouse skin tumorigenesis. Carcinogenesis 2008;29:1108-14

24. Kim DJ, Angel JM, Sano S, DiGiovanni J. Constitutive activation and targeted disruption of signal transducer and activator of transcription 3 (Stat3) in mouse epidermis reveal its critical role in UVB-induced skin carcinogenesis. Oncogene 2009;28:950-60

25. Tarutani M, Itami S, Okabe M, et al. Tissue-specific knockout of the mouse Pig-a gene reveals important roles for GPI-anchored proteins in skin development. Proc Natl Acad Sci U S A 1997;94:7400-5

26. Ehrenreiter K, Piazzolla D, Velamoor V, et al. Raf-1 regulates Rho signaling and cell migration. J Cell Biol 2005;168:955-64

27. Chiarle R, Simmons WJ, Cai H, et al. Stat3 is required for ALK-mediated lymphomagenesis and provides a possible therapeutic target. Nat Med 2005;11:623-9

28. Fuchs E. Keratins and the skin. Annu Rev Cell Dev Biol. 1995;11:123-53

29. Byrne C, Fuchs E. Probing keratinocyte and differentiation specificity of the human K5 promoter in vitro and in transgenic mice. Mol Cell Biol 1993;13:3176-90

30. Ramirez A, Bravo A, Jorcano JL, Vidal M. Sequences 5' of the bovine keratin 5 gene direct tissue- and cell-type-specific expression of a lacZ gene in the adult and during development. Differentiation 1994;58:53-64

31. Yin W, Cheepala S, Roberts JN, Syson-Chan K, DiGiovanni J, Clifford JL. Active Stat3 is required for survival of human squamous cell carcinoma cells in serum-free conditions. Mol Cancer 2006;5:15

32. Santarosa M, Ashworth A. Haploinsufficiency for tumour suppressor genes: when you don't need to go all the way. Biochim Biophys Acta 2004;1654:105-22

33. McKusick VA. OMIM^{TM}: OMIM™: Online Mendelian Inheritance in Man. http://www.ncbi.nlm.nih.gov/Omim/

34. Seidman JG, Seidman C. Transcription factor haploinsufficiency: when half a loaf is not enough. J Clin Invest 2002;109:451-5

35. Bollrath J, Phesse TJ, von Burstin VA, et al. gp130-mediated Stat3 activation in enterocytes regulates cell survival and cell-cycle progression during colitis-associated tumorigenesis. Cancer Cell 2009;15:91-102

Figure legends

Figure 1. Keratinocyte-specific disruption of the Stat3 gene by the Cre-*LoxP* system. A, a partial genomic map of the Stat3 gene before and after Cre-mediated disruption. The exons to be excised (16-21, solid boxes) were flanked by two identically oriented LoxP sites (dotted triangles). The three primers indicated, A, B and C, were used for the detection of wild-type (wt), floxed (LoxP), and disrupted (null) Stat3 alleles respectively. **B**, allele specific PCR analysis performed on tail (T) and keratinocyte (KC) genomic DNA preparations; the primers used are described in the M&M (M, Quick-Load® 100 bp DNA Ladder). **C,** analysis of Stat3 protein levels in epidermal lysates (30 μg) pooled from three animals for each genotype. β-actin was used to control for equal loading.

Figure 2. **Stat3 deletion in keratinocytes causes retarded development and epidermal defects. A,** appearance of $Stat3^{+/+}$, $Stat3^{+/-}$, and $Stat3^{-/-}$ mice not expressing (upper part) or expressing (lower part) HPV8 early genes at postnatal day 25. Scale bars, 1cm. **B,** histology of mouse skin, stained with H&E, obtained from non-lesional areas of the mice shown in panel *A*. Scale bars, 50μm. **C,** immunohistochemical staining of PCNA in serial sections obtained from the skin specimens shown in panel *B*. Dark brown color indicates PCNA-positive cells; blue color indicates nuclear counterstaining. Scale bars, 25μm. **D,** immunohistochemistry of serial sections of the skin specimens shown in panel *B* stained for Stat3. Dark brown color indicates positive cells; blue color indicates nuclear counterstaining. Scale bars, 25μm. **E**, quantification of epidermal thickness. Each value is the mean ± *SD* from 4 mice. There were six skin sections per mouse. Two sections were scored for a total of at least six views. (***p<0.001, two-way ANOVA followed by Bonferroni post test). ND, not detectable. **F**, quantification of PCNA-positive cells. An average of at least four mice per genotype was used to calculate the percentage (mean ± *SD)* (***p<0.001, **p<0.01, two-way ANOVA followed by Bonferroni post test). ND, not detectable.

Figure 3. **Kaplan-Meier plot of the tumor-free state as a function of time in $Stat3^{+/+}$:HPV8 and $Stat3^{+/-}$:HPV8 mice.** Mice were monitored twice weekly over a period of 52 weeks and for at least 12 weeks after birth. The indicated *p* value refers to Log-rank test.

Figure 4. HPV8-induced skin cancer progression is impaired in $Stat3^{+/-}$ transgenic mice. A, gross appearance of $Stat3^{+/+}$:HPV8 mice at 6 weeks of age with benign papillomas that convert into carcinomas by 15 weeks. On the right, a $Stat3^{+/-}$:HPV8 mouse at 20 weeks of age showing benign papillomas. Representative H&E-stained skin lesion sections derived from the photographed mice are shown. Scale bars, 100μm. Immunohistochemistry for pStat3 of serial sections of the skin specimens stained by H&E. Dark brown color indicates positive cells; blue color indicates nuclear

counterstaining. Scale bars, 25μm. **B**, quantification of pStat3-positive cells. An average of at least three mice per group was used to calculate the percentage (mean ± *SD)* (***p<0.001, **p<0.01, one-way ANOVA followed by Bonferroni post test). **C**, analysis of Stat3 and pStat3 protein levels in nonlesional versus tumor epidermal lysates from $Stat3^{+/+}$ and $Stat3^{+/-}$ mice, transgenic or nontransgenic for HPV8 oncoproteins. Lysates (30 μg) were pooled from three animals for each genotype. β-actin was used to control for equal loading.

Figure 5. Expression of PCNA, keratin 10 (K10), and keratin 5 (K5) in skin lesions from $Stat3^{+/-}$:HPV8 and $Stat3^{+/+}$:HPV8 mice Immunohistochemistry of serial sections of the skin specimens shown in Figure 4, panel A stained for PCNA, K10, AND K5. Dark brown color indicates positive cells; blue color indicates nuclear counterstaining. Scale bars, 25μm. The arrow indicates an island of K5-positive keratinocytes in the dermis.

Figures

Figure 1

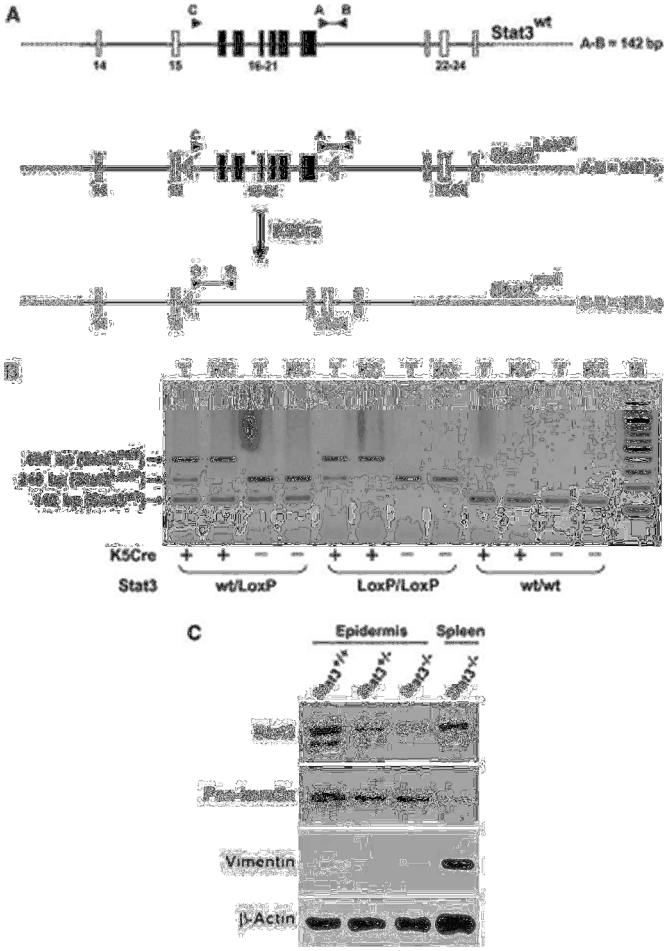

Figure 2

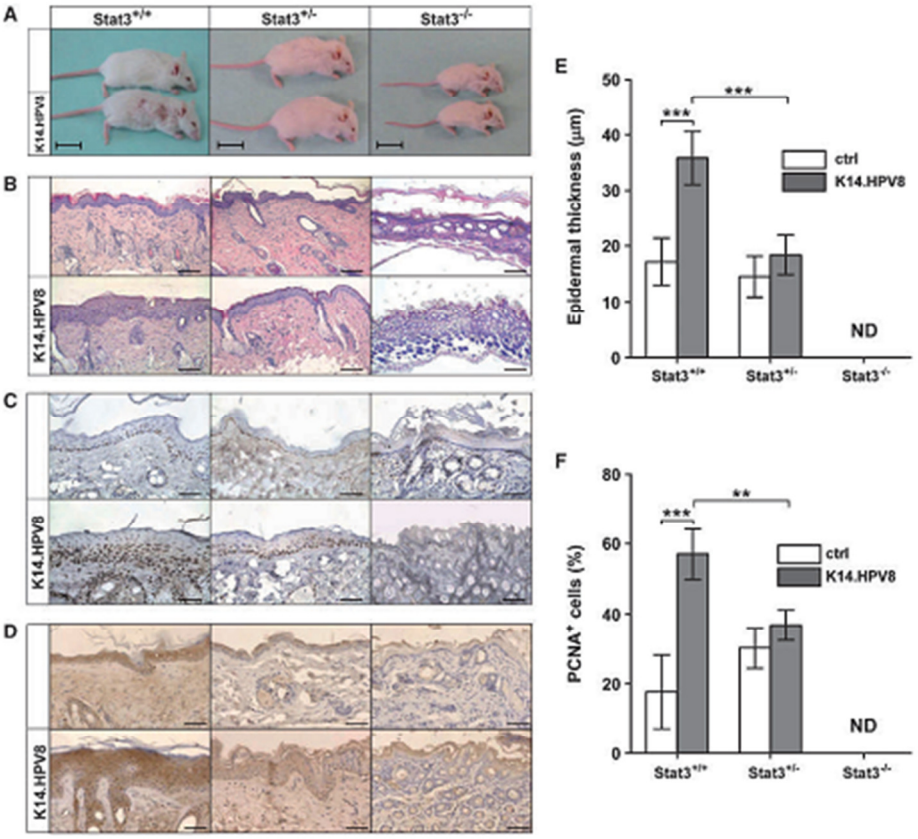

Figure 3

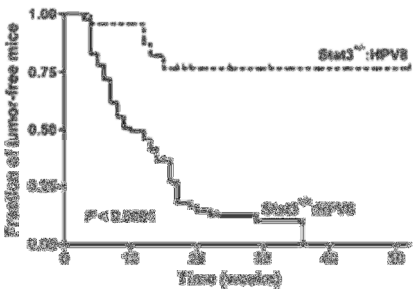

Figure 4

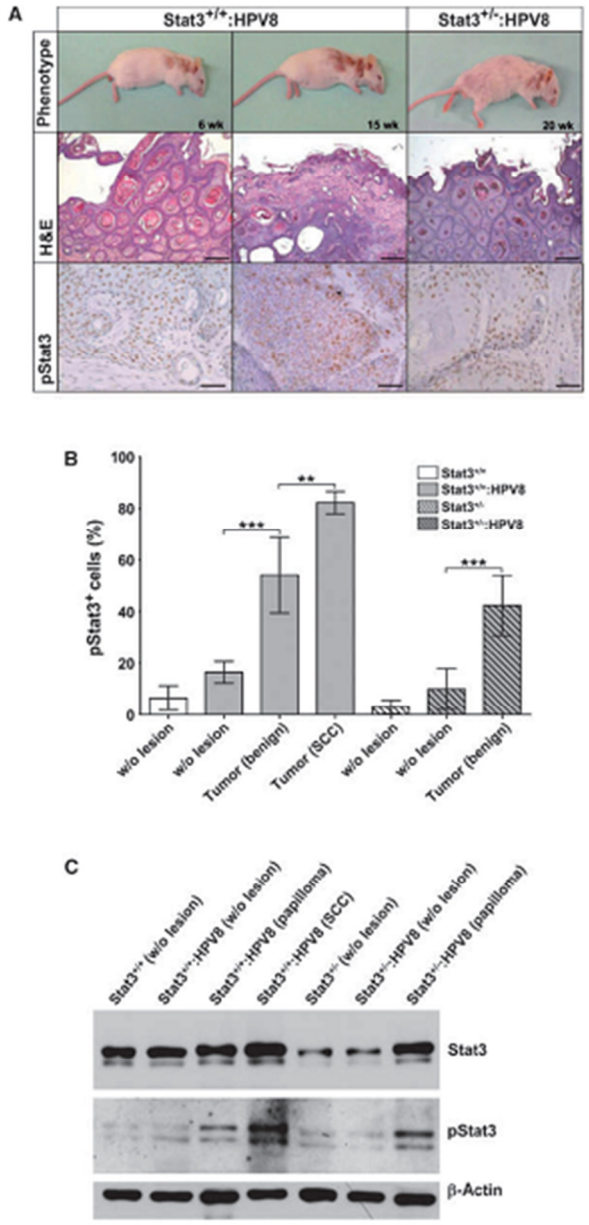

Figure 5

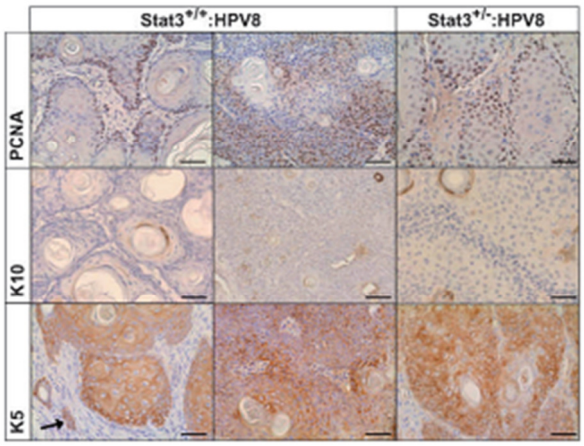

Tables

Table 1. Genotypes of animals

Genotypes	Aliases
K5Cre:Stat3$^{LoxP/LoxP}$/K14-HPV8	Stat3$^{-/-}$:HPV8
K5Cre:Stat3$^{wt/LoxP}$/K14-HPV8	Stat3$^{+/-}$:HPV8
K5Cre:Stat3$^{wt/wt}$/K14-HPV8	Stat3$^{+/+}$:HPV8
Stat3$^{LoxP/LoxP}$/K14-HPV8	
Stat3$^{wt/LoxP}$/K14-HPV8	
Stat3$^{wt/wt}$/K14-HPV8	
K5Cre:Stat3$^{LoxP/LoxP}$	Stat3$^{-/-}$
K5Cre:Stat3$^{wt/LoxP}$	Stat3$^{+/-}$
K5Cre:Stat3$^{wt/wt}$	Stat3$^{+/+}$
Stat3$^{LoxP/LoxP}$	
Stat3$^{wt/LoxP}$	
Stat3$^{wt/wt}$	

Table 2. Summary of tumor characteristics in the skin

Genotypes	at 12 wk of age			at 52 wk of age			Average age of tumor onset
	No. mice	Mice with tumor	Mice with multiple tumors	No. mice	Mice with tumor	Mice with multiple tumors	
Stat3$^{+/+}$	125	0	0	110	0	0	NA
Stat3$^{+/-}$	44	0	0	37	0	0	NA
Stat3$^{-/-}$	19	NA	NA	13	NA	NA	NA
Stat3$^{+/+}$:HPV8	81	44	37	65	65	55	10.1
Stat3$^{+/-}$:HPV8	23	3*	3†	11	5*	4†	11.3‡
Stat3$^{-/-}$:HPV8	17	NA	NA	11	NA	NA	NA

Abbreviation: NA, data not applicable.

*Partial loss of Stat3 in the skin resulted in a significant reduction of tumor incidence in Stat3+/ :HPV8 in comparison with Stat3+/+:HPV8 transgenic mice, at both week 12 ($P = 0.0006$) and week 52 ($P < 0.0001$).

†In tumor-bearing mice, partial loss of Stat3 in the skin did not result in a significant change of multiple tumor incidence in Stat3+/– :HPV8 in comparison with Stat3+/+ :HPV8 transgenic mice ($P > 0.05$, at both weeks 12 and 52).

‡Partial loss of Stat3 in the skin resulted in a not significant delayed time of tumor onset in Stat3+/– :HPV8 in comparison with Stat3+/+ :HPV8 transgenic mice.